The American Journal of Pathology, Vol. 174, No. 3, March 2009

DOI: 10.2353/ajpath.2009.080262

Gastrointestinal, Hepatobiliary and Pancreatic Pathology

Gallbladder Epithelial Cells that Engraft in Mouse Liver Can Differentiate into Hepatocyte-Like Cells

Sum P. Lee, Christopher E. Savard, and Rahul Kuver

From the Division of Gastroenterology, Department of Medicine, University of Washington and the Puget Sound Veterans Affairs Health Care System, Seattle Division, Seattle, Washington

We tested the hypothesis that well-differentiated gallbladder epithelial cells (GBECs) are capable of engrafting and surviving in murine liver and acquire phenotypic characteristics of hepatocytes. GBECs isolated from transgenic mice that constitutively express green fluorescent protein (GFP) were either cultured before transplantation or transplanted immediately following isolation. Recipient mice with severe-combined immunodeficiency underwent retrorsine treatment and either partial hepatectomy before transplantation or carbon tetrachloride treatment following transplantation. From 1 to 4 months following transplantation, the livers of recipient mice contained discrete colonies of GFP$^+$ cells. Most GFP$^+$ cells surrounded vesicles, were epithelial cell-like in morphology, and expressed the biliary epithelial markers cytokeratin 19 and carbonic anhydrase IV. Subpopulations of GFP$^+$ cells resembled hepatocytes morphologically and expressed the hepatocyte-specific markers connexin-32 and hepatic nuclear factor-4α, but not cytokeratin 19 or carbonic anhydrase IV. At 4 months, cells in GFP$^+$ colonies were not actively proliferating as determined by proliferating cell nuclear antigen expression. Thus, GBECs are capable of engrafting and surviving in damaged mouse livers, and some can differentiate into cells with hepatocyte-like features. These findings suggest that environmental cues in the recipient liver are sufficient to allow a subpopulation of donor GBECs to differentiate into hepatocyte-like cells in the absence of exogenous transcriptional reprogramming. GBECs might be used as donor cells in a cell transplantation approach for the treatment of liver disease. ***(Am J Pathol 2009, 174:842–853; DOI: 10.2353/ajpath.2009.080262)***

Hepatocytes, intrahepatic cholangiocytes, extrahepatic biliary epithelial cells, and gallbladder epithelial cells (GBEC) share embryologic origins. This common ancestry has implications in adulthood. For example, cells within the adult liver with pluripotential capacity, such as oval cells, are able to differentiate into either hepatocytes or cholangiocytes when hepatocyte regeneration is blocked.[1–3] Furthermore, plasticity between cell lineages has been demonstrated with respect to intrahepatic cholangiocytes and hepatocytes.[4–6] Whether this lineage plasticity is mediated predominantly by cells with stem cell properties, or whether terminally differentiated cells of one lineage are able to directly differentiate into another lineage (ie, undergo transdifferentiation) remains unsettled.[7–9] Recently, we showed that meticulously isolated and rigorously characterized terminally differentiated GBEC cultured under defined *in vitro* conditions could acquire hepatocyte-like properties, such as the ability to synthesize bile acids and take up low-density lipoprotein, without expression of oval cell or hematopoietic stem cell markers.[10] Thus, cells of biliary lineage resident in the extrahepatic compartment retained the capacity to acquire hepatocyte-like phenotypic characteristics when exposed to certain environmental conditions.

While hepatocyte transplantation has been intensively investigated using various animal models[11,12] (and also recently in the clinical setting[13,14]) with varying degrees of success, the use of this technique in humans is limited by the availability and suitability of donor cells.[15,16] Xenotransplantation of porcine hepatocytes has shown promise,[17] but this approach carries immunological and infectious risks. If terminally differentiated GBEC are able to acquire hepatocyte-like phenotypic characteristics, then a logical question is whether such cells might be able to repopulate damaged liver. We reasoned that GBEC might serve as ideal extrahepatic donor cells as

Supported by Grant DK-061157 from the National Institute of Diabetes and Digestive and Kidney Diseases and a Merit Review Award from the Department of Veterans Affairs.

Accepted for publication November 18, 2008.

Current address of S.P.L. is LKS Faculty of Medicine, University of Hong Kong, Sassoon Rd., Hong Kong.

Address reprint requests to Rahul Kuver, Division of Gastroenterology, Box 356424, University of Washington, 1959 NE Pacific St., Seattle, WA 98195. E-mail: kuver@u.washington.edu.

they could be isolated and cultured from the same patient. Donor cells could be expanded *in vitro* before transplantation, thereby potentially enhancing the chances of successful engraftment. Furthermore, if such cells could acquire functional characteristics of hepatocytes, they could be used to repopulate damaged livers. Successful transplantation of GBEC that had been cultured repeatedly before engraftment would also support the concept of transdifferentiation of a terminally differentiated cell population. We therefore set out to test this concept in a murine model wherein genetically marked GBEC were transplanted into recipient immune-deficient mice with damaged livers.

Materials and Methods

GBEC Isolation

Donor mice C57BL/6J mice, heterozygously expressing green fluorescent protein (GFP mice, strain C57BL/6-TgN[lqsb]ACTbEGFP]1Osb/J) were purchased from Jackson Labs (Bar Harbor, ME). To obtain freshly isolated donor GBEC, male and female adult GFP mice, weighing 15 to 30 g, were anesthetized using isoflurane and immediately euthanized by cervical dislocation. The abdomen was exposed and the gallbladder (GB) separated from the liver and bile duct using forceps. Excess tissue was removed and the GB placed in Eagle's Minimal Essential Media on ice. Each GB was inspected using a dissecting microscope at ×4 magnification. Any non-GB tissues, including liver and adipose tissue, were completely removed using a scalpel. Each GB was cut in half, placed into 50 ml cold PBS, and washed five times with cold PBS then transferred to 60-mm tissue culture plates. Five ml trypsin/EDTA (2.5 g/L and 1 g/L respectively) were added and samples were incubated at 37°C in a 5% CO_2 incubator for 45 minutes with intermittent shaking. After 45 minutes, the trypsin was inactivated with media containing 10% fetal bovine serum and the released cells were passed through a 100-μm mesh to remove large GB fragments. Live cell counts were performed using trypan blue and a hemacytometer. The average live cell harvest was $5.5 \times 10^5 \pm 1.2 \times 10^5$ ($n = 9$) cells per GB. Cells were pelleted at 300 × *g* for 6 minutes and then resuspended in sterile saline (~75 μl per sample) and stored on ice until transplantation. Harvested cells from five mouse GBs were pooled for each recipient mouse. All animal protocols were reviewed and approved by the Institutional Animal Care and Use Committee.

GFP-positive GBEC (GFP^+GBEC) were also isolated for long-term culturing using a previously described protocol.[18] Cultured GFP^+GBEC can be repeatedly passaged and maintain characteristics of normal well-differentiated GBEC and GFP expression.

Recipient mice had severe combined immune deficiency (SCID mice; B6.CB17-$Prkdc^{scid}$/SzJ from Jackson Labs). They were treated with retrorsine, a pyrrolizidine alkaloid that blocks the hepatocyte cell cycle, before surgery.[19] Retrorsine stock was 20 mg/ml in 100% ethanol. For injection, stock was diluted with sterile PBS to 4 mg/ml. SCID mice received retrorsine 50 mg/kg i.p., followed by a second dose of 30 mg/kg, 2 weeks thereafter. Cell transplantation was performed 2 to 4 weeks after final retrorsine treatment.

Surgical Procedure

Anesthesia was induced with 4% isoflurane, supplied with a calibrated vaporizer with 1 L O_2/min, and maintained with 0.5% to 1.5% isoflurane with 1 L O_2/min. Buprenorphine at 0.1 mg/kg was given as an analgesic at the time of laparotomy. For mice undergoing partial hepatectomy, 2/3 of the liver was removed. Freshly isolated cells from the donor GFP^+ mice GBs or cultured GFP^+GBEC were injected into the spleen of recipient mice using a 27 gauge needle (~75 μl per mouse); $3.2 \times 10^6 \pm 1.0 \times 10^6$ ($n = 9$) freshly isolated cells or $3.1 \times 10^6 \pm 2.0 \times 10^6$ ($n = 11$) cultured cells were injected per mouse. The abdominal wall was sutured and the skin closed with wound clips. Two to four weeks after transplantation, the recipient mice that did not undergo partial hepatectomy were given an intraperitoneal dose of carbon tetrachloride (0.4 ml/kg). CCl_4 was diluted 1:10 with mineral oil before injection. CCl_4 injection was repeated twice at weekly intervals. Mice with partial hepatectomy, with a few exceptions, did not receive CCl_4 treatment. At intervals ranging from 1 month to 4 months following surgery, mice were euthanized by cervical dislocation following isoflurane anesthesia. The livers were removed and snap frozen in optimal cutting temperature compound (Tissue-Tek, Torrance, CA) using liquid nitrogen. Frozen tissue was cut sequentially into 10 μm sections and stored in a −70°C freezer.

GFP Fluorescence Analysis

Every 20th slide was covered with a glass slip with Aquamount aqueous mounting media containing Hoechst 33342 nuclear dye (1 μg/ml). A Nikon Eclipse fluorescence microscope was used with fluorescein isothiocyanate (FITC) filters (excitation 460 to 500 nm) to view GFP^+ tissue and UV/4,6-diamidino-2-phenylindole filters (excitation 330 to 380 nm) to view nuclei. To confirm that fluorescence was due to GFP, slides that had been incubated with a primary rabbit anti-GFP antibody (Invitrogen, Carlsbad, CA), followed by a rhodamine-conjugated donkey anti-rabbit IgG secondary antibody (Santa Cruz), were viewed using tetramethylrhodamine B isothiocyanate (TRITC) filters (excitation 530 to 550 nm). Serial images were then obtained using fluorescence microscopy with specific filters (FITC for GFP fluorescence; TRITC for anti-GFP antibody immunofluorescence) on the same slide. Images were captured digitally (Qimaging) and processed using ImagePro software (Media Cybernetics, Bethesda, MD).

Quantitation of GFP$^+$ Cells in Recipient Mouse Livers

Frozen tissue was sectioned using a cryostat and at least 300 sections made for each liver. Each 10-μm liver section was adhered to a glass slide and stored in sequential order. GFP$^+$ regions were assessed as follows on four slides randomly selected from each liver. For each slide, digital images were taken of four randomly selected low power fields ($\times$40 original magnification; 6.8 mm^2 total area/image) using both the FITC and TRITC filters on a Nikon Eclipse Fluorescent microscope. NIH Image J density software was used to analyze each FITC image. The threshold adjust tool was used to highlight green fluorescent areas, which were measured and expressed as a percentage of the total liver area. The FITC images also had varying degrees of non-GFP autofluorescence, detectable at all visible-light excitation wavelengths used, that was highlighted along with true GFP fluorescence. Therefore, the corresponding TRITC images were used in the same manner to calculate the percentage of non-GFP autofluorescence, which was subtracted from the total fluorescent area to obtain the percentage of true GFP$^+$ fluorescence. The mean $\pm$ SD of these 16 measures (four low power fields for each of four slides) represented the proportion of GFP$^+$ cells of GBEC origin in the recipient liver.

Morphology

Cell morphology was evaluated following H&E staining. GFP$^+$ areas seen under the fluorescent microscope were identified on the H&E-stained section, and these paired images were captured digitally.

Immunofluorescence

Tissue sections were thawed to room temperature, then fixed with formalin for 3 minutes. After washing, the tissue was blocked using PBS containing 10% donkey or goat serum (depending on the source of secondary antibody being used) for 1 hour. Primary antibodies were: goat anti-aldolase B, hepatocyte nuclear factor-4α (HNF-4α), cytokeratin 19 (CK19), and carbonic anhydrase IV (all from Santa Cruz), used at 1:50 dilution. Primary antibodies were diluted in PBS with 2% serum and incubated at room temperature for 1 hour. Slides were then incubated with AlexaFluor 633-donkey anti-goat IgG at 10 μg/ml for 1 hour. After washing, slides were mounted with Aquamount. The Alexa 633 label was visualized using the Texas Red filter (excitation 532 to 587 nm). Slides were also analyzed using a Leica TCS-SP confocal microscope.

For proliferating cell nuclear antigen (PCNA) staining, 10 μm liver sections were blocked with 10% goat serum in PBS. Primary antibody was a rabbit polyclonal anti-PCNA antibody (Bethyl Labs, Montgomery, TX) diluted 1:100 in 2% goat serum/PBS for 1 hour. After washing, sections were treated with goat anti-rabbit IgG-labeled with Alexa Fluor 663 (Invitrogen) at 10 μg/ml for 1 hour.

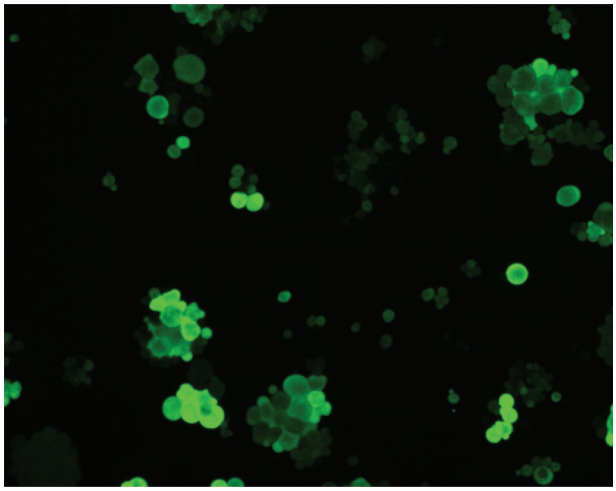

Figure 1. Trypsinized donor GFP$^+$GBEC in suspension, as viewed with fluorescence microscopy. Magnification = original $\times$200. Cells shown were cultured and passaged eight times before analysis. Freshly isolated GFP$^+$GBEC showed the same typical green fluorescence.

After washing, the tissue was overlaid with a coverslip using Aquamount mounting media and viewed using a Nikon Eclipse fluorescence microscope. Digital images were captured using both the FITC and the Texas Red filter sets. Positive control samples were actively dividing cultured mouse GBEC. Negative controls were sections in which the primary anti-PCNA antibody was omitted.

Results

GFP$^+$GBEC Engraft in SCID Mouse Liver in Distinct Colonies

Cultured and freshly isolated GBEC from GFP mice exhibited green fluorescence at the expected wavelengths (Figure 1). GFP$^+$GBEC were injected into the spleens of SCID mice that had been pre-treated with retrorsine, with subsequent CCl_4 treatment. GFP$^+$ cells were found in discrete colonies scattered throughout the recipient liver as areas of green fluorescence that were more prominent than background autofluorescence (Figure 2A, arrows). Vesicular structures were evident even at low power (top arrow, Figure 2A). Distinct GFP$^+$ cells within these fluorescent colonies were evident under higher magnification (Figure 2, B and C). While the majority of the GFP$^+$ cells were small, epithelial cell-like, and bordered the vesicular structures (dashed arrows in Figure 2, C and E), a subset of GFP$^+$ cells were much larger in size and resembled hepatocytes (solid arrows in Figure 2, C and E), with large round nuclei and abundant cytoplasm. Well-demarcated borders of these GFP$^+$ colonies were seen in GFP-nuclear stain overlay images (Figure 2, D and E). Note that the majority of nuclei are in GFP-negative regions in the recipient liver. GFP$^+$ colonies were found from 1 to 4 months from the time of transplantation. Similar findings were seen in mice that were treated with CCl_4 in lieu of partial hepatectomy. Mice in which either partial hepatectomy or CCl_4 treatment was omitted, or mice that did

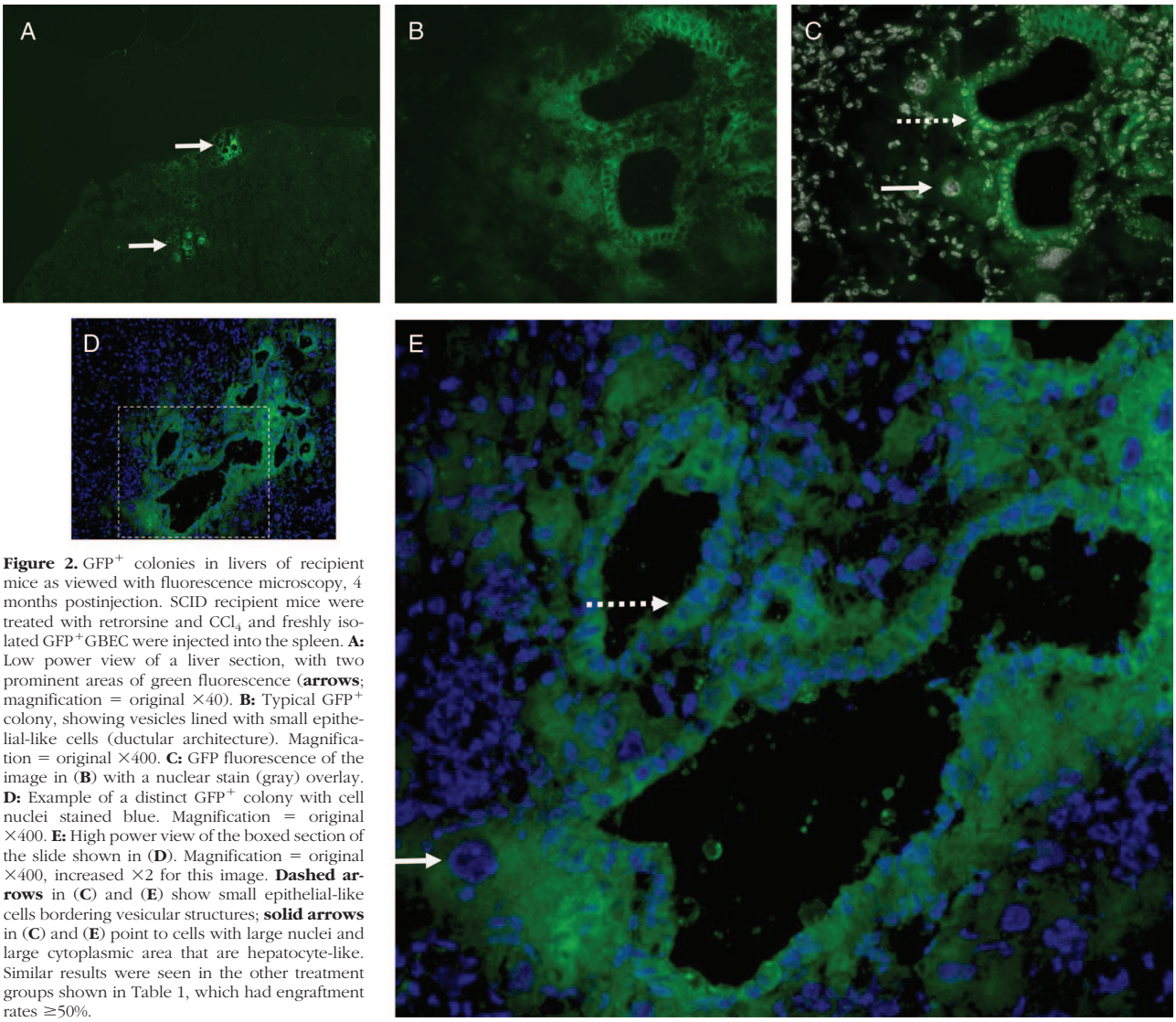

Figure 2. GFP^+ colonies in livers of recipient mice as viewed with fluorescence microscopy, 4 months postinjection. SCID recipient mice were treated with retrorsine and CCl_4 and freshly isolated GFP^+GBEC were injected into the spleen. **A:** Low power view of a liver section, with two prominent areas of green fluorescence (**arrows**; magnification = original ×40). **B:** Typical GFP^+ colony, showing vesicles lined with small epithelial-like cells (ductular architecture). Magnification = original ×400. **C:** GFP fluorescence of the image in (**B**) with a nuclear stain (gray) overlay. **D:** Example of a distinct GFP^+ colony with cell nuclei stained blue. Magnification = original ×400. **E:** High power view of the boxed section of the slide shown in (**D**). Magnification = original ×400, increased ×2 for this image. **Dashed arrows** in (**C**) and (**E**) show small epithelial-like cells bordering vesicular structures; **solid arrows** in (**C**) and (**E**) point to cells with large nuclei and large cytoplasmic area that are hepatocyte-like. Similar results were seen in the other treatment groups shown in Table 1, which had engraftment rates ≥50%.

not receive retrorsine, showed no GFP^+ colonies in their livers. These results were replicated using GFP^+GBEC that were cultured for several passages, rather than freshly isolated, with the exception that preparation of recipient liver with partial hepatectomy alone did not lead to engraftment of cultured GFP^+GBEC. All recipient mice found to have GFP^+ cells within their livers survived without adverse sequelae. The findings are summarized in Table 1.

Differentiating GFP Fluorescence from Background Autofluorescence in Recipient Mouse Livers

Faint background fluorescence was seen in all livers examined, even though distinct areas of bright green fluorescence were readily apparent even at low magnification (Figure 2A, arrows). To confirm that GFP fluores-

Table 1. Summary of Experiments

Recipient mouse type	Retrorsine	Donor cell	Recipient liver treatment	Post-transplant duration (months)	# Mice with GFP^+ cells	# Mice Analyzed	% Recipient mice with GFP^+ cells
SCID	yes	Freshly isolated GFP^+GBEC	CCl_4	4	5	5	100%
SCID	yes	Freshly isolated GFP^+GBEC	CCl_4	2	3	3	100%
SCID	yes	Freshly isolated GFP^+GBEC	PH	4	3	3	100%
SCID	yes	Cultured GFP^+GBEC	PH & CCl_4	4	2	2	100%
SCID	yes	Cultured GFP^+GBEC	CCl_4	4	1	2	50%
SCID	yes	Cultured GFP^+GBEC	PH	1 & 4	0	2	0%
SCID	no	Freshly isolated GFP^+GBEC	PH	6	0	3	0%

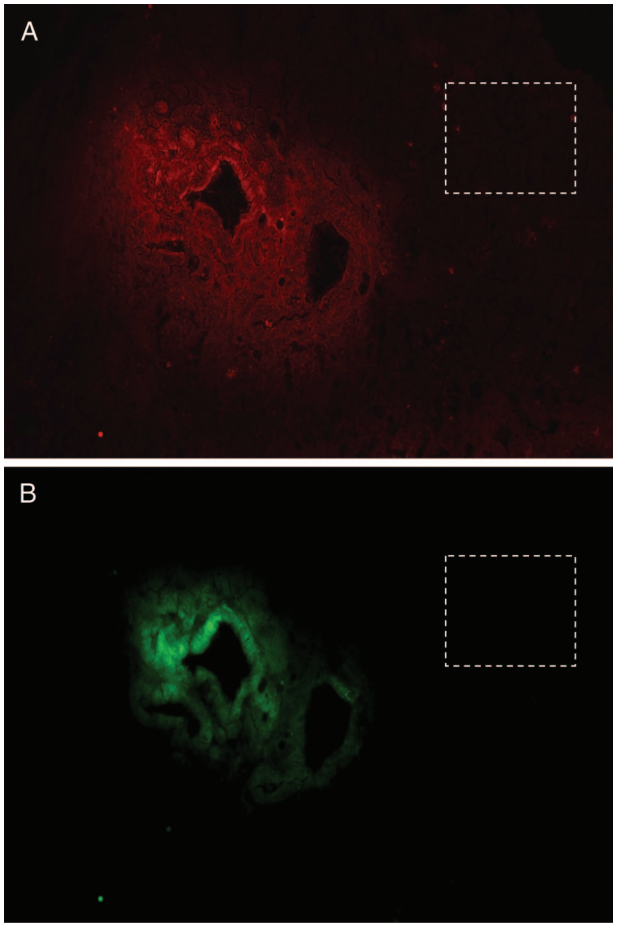

Figure 3. Comparison, on the same section, of fluorescence signals from staining with an anti-GFP antibody and a TRITC-conjugated secondary antibody (TRITC filter **A**) vs. using direct GFP fluorescence (FITC filter, **B**). Magnification = original ×400. Note that signal intensity is weaker with the FITC filter compared with the TRITC filter due to the loss of signal associated with incubation with primary and secondary antibodies before fluorescence microscopy. The boxed area shows a region of recipient mouse liver that is GFP negative by both methods of detection. Mice were treated as in Figure 2. Similar results were seen in the other treatment groups shown in Table 1, which had engraftment rates ≥50%.

cence was truly due to GFP and not due to background autofluorescence, we also used an anti-GFP antibody in an indirect immunofluorescence protocol. Figure 3, A and B shows a representative liver section containing a GFP$^+$ colony detected by TRITC filter for anti-GFP antibody immunofluorescence (Figure 3A) and FITC filter for GFP fluorescence (Figure 3B). As compared with adjacent unstained sections, GFP fluorescence using the FITC filter faded appreciably, due to the extra time associated with the immunofluorescence staining; hence, the signal intensity in Figure 3B is lower than in Figure 3A. Nevertheless, there was excellent correlation in the areas in which fluorescence was detected. GFP-negative regions in sections labeled with an anti-GFP antibody and a rhodamine-labeled secondary antibody were also negative when viewed with a FITC filter (boxed areas in Figure 3, A and B).

We performed two additional control experiments to show that the green fluorescence signal was specific for GFP$^+$ colonies and not due to background autofluorescence in recipient mouse liver. First, true GFP$^+$ cells did not fluoresce when viewed through the TRITC or Texas Red filters in the absence of a rhodamine- or Alexa 633-conjugated secondary antibody. Second, in Hoechst 33342-stained liver sections, photobleaching with UV light dramatically attenuated GFP fluorescence, an effect that was not seen with background autofluorescence. We confirmed the specificity of GFP fluorescence signals subsequently on all experiments by using these techniques.

Quantitation of GFP$^+$ Cells in Recipient Mouse Livers

Quantitation of GFP$^+$ areas was performed for five different retrorsine-treated SCID mouse livers, harvested 4 months after injection with freshly isolated GFP$^+$GBEC

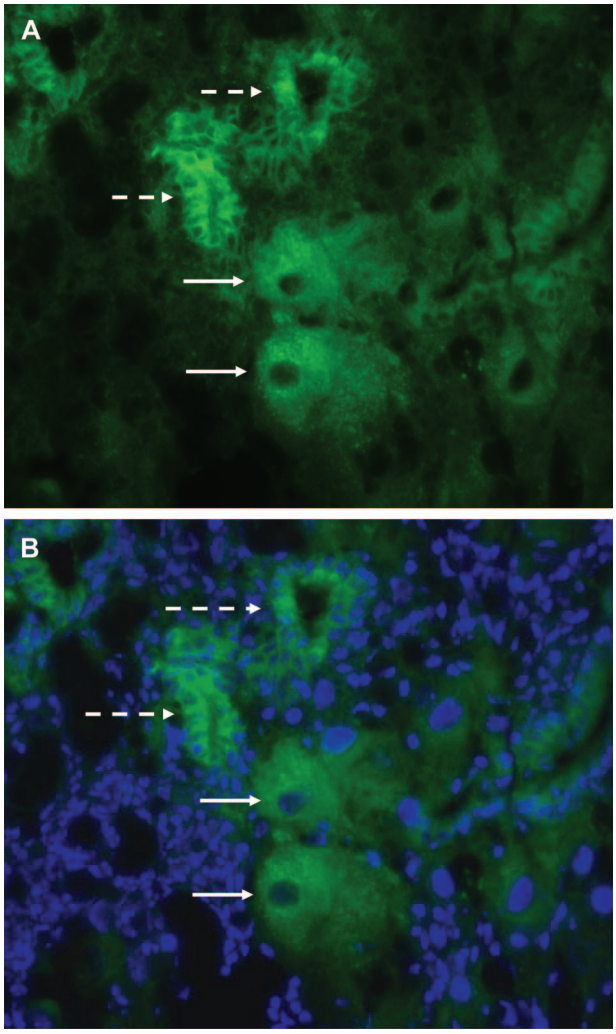

Figure 4. Example of a GFP$^+$ colony exhibiting mixed histological architecture composed of small epithelial-like cells lining vesicular structures (ductular morphology) and larger cells that resemble hepatocytes (**A:** GFP fluorescence; **B:** GFP fluorescence with nuclear stain overlay). **Dashed arrows** point to small epithelial-like cells with ductular morphology and **solid arrows** point to larger hepatocyte-like cells. Mice were treated as in Figure 2. Similar results were seen in the other treatment groups shown in Table 1, which had engraftment rates ≥50%. Magnification = original ×400.

followed by CCl_4 treatment. From these five experiments, we obtained estimates of the proportion of true GFP^+ cells per recipient liver. The results showed 1.46%, 0.37%, 5.77%, 1.26%, and 0.86% of cells in these five livers were true GFP^+ (M = 1.94%, SD = 2.18%).

Varied Morphological Features of GFP^+ Cells in Recipient Mouse Livers

Most GFP^+ colonies consisted of vesicles lined with a single layer of small epithelial-like cells (Figure 2, B and

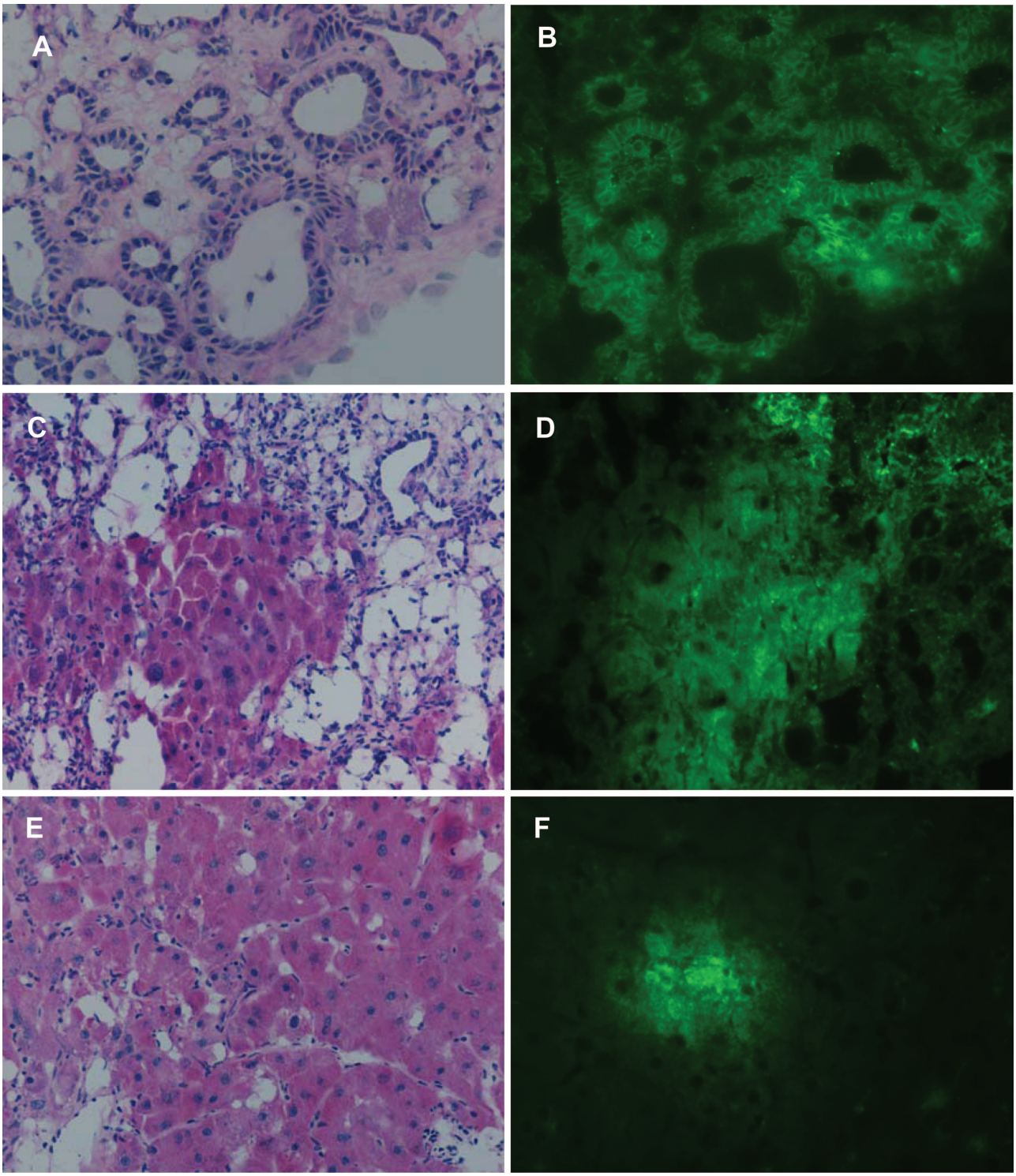

Figure 5. Comparison of adjacent sections of recipient mouse liver, fixed and stained with H&E, and viewed with optical microscopy (**A, C, E**), or unfixed and viewed under fluorescence microscopy to highlight GFP^+ regions (**B, D, F**). Magnification = original ×400. (**A**) and (**B**) show a region with predominantly ductular morphology; (**C**) and (**D**) show a region with mixed epithelial cell and hepatocyte-like morphology; and (**E**) and (**F**) show a region with predominantly hepatocyte-like morphology. Mice were treated as in Figure 2. Similar results were seen in the other treatment groups shown in Table 1, which had engraftment rates ≥50%.

C). Larger GFP$^+$ cells that resembled hepatocytes were also seen (solid arrows, Figure 2, C and E). The nuclear-stained sections (Figure 2, C–E) reveal the integrated nature of these GFP$^+$ colonies; there is no abrupt break in the nuclear architecture between the GFP$^+$ and GFP$^-$ areas. The similarity of the nuclear staining pattern in GFP$^+$ areas with GFP$^-$ areas suggests that cellular processes that would manifest as changes in nuclear morphology, such as apoptosis or tumor formation, were not occurring in GFP$^+$ regions. As shown in Figure 4, A and B, a subset of GFP$^+$ colonies possessed mixed cellular morphology, with both small epithelial cells lining vesicles (dashed arrows), as well as larger cells with abundant cytoplasm and large, round nuclei, which resembled hepatocytes (solid arrows).

On H&E-stained sections, GFP$^+$ colonies contained either predominantly small epithelial-like cells (ductular morphology) (Figure 5A), or a mixed architecture containing both small epithelial-like cells and larger cells with hepatocyte-like morphology (Figure 5C). Other colonies were predominantly hepatocyte-like in morphology (Figure 5E). Fluorescence microscopy performed on adjacent sections showed distinct GFP$^+$ areas, with a strong GFP signal noted in cells exhibiting epithelial cell-like and hepatocyte-like morphology (Figure 5, B, D, and F). In areas where GFP$^+$ hepatocyte-like cells predominated, these cells appeared to be integrated into the underlying architecture of native hepatocytes in the recipient livers (Figure 5E compared with 5F).

SCID mouse livers that had been treated with retrorsine and either partial hepatectomy or CCl_4, but which had not been injected with GFP$^+$GBEC, were also assessed for morphological changes using H&E staining. Patchy histological damage resulted (Figure 6, A–C) that was more pronounced following CCl_4 treatment than following partial hepatectomy. The severity of the liver damage was not uniform and histologically normal areas were also seen (not shown). Most importantly, the distinctive vesicles lined with epithelial-like cells were not observed in livers that did not undergo GFP$^+$GBEC transplantation (compare Figure 6 to Figures 2–5).

As a nuclear marker of cell proliferation, PCNA immunofluorescence was uniformly undetectable in GFP$^+$ areas in six recipient mouse livers 4 months after transplantation (Figure 7, A and B). Actively dividing subconfluent cultured wild-type mouse GBEC, used as a positive control, displayed prominent nuclear staining for PCNA (Figure 7C).

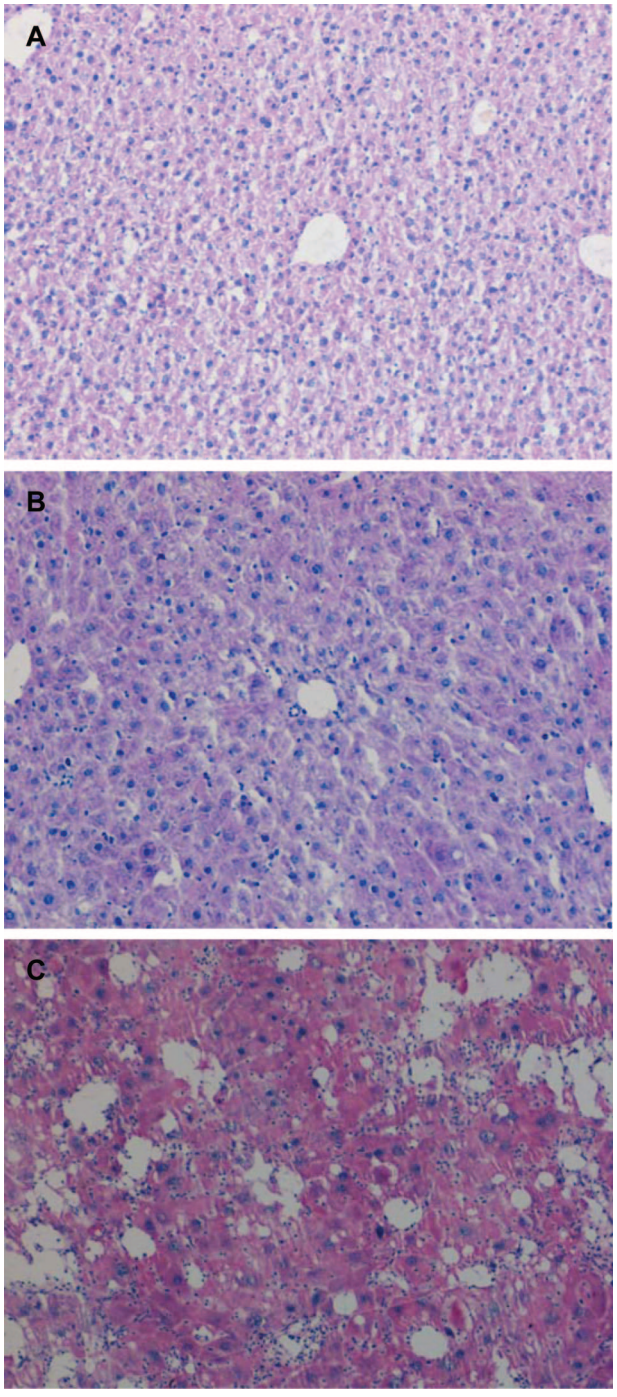

Figure 6. Histology of untreated SCID mouse liver (**A**), of SCID mouse liver treated with retrorsine and then subjected to partial hepatectomy (**B**), and of SCID mouse liver treated with retrorsine followed by CCl_4 (**C**). These mice were not injected with GFP$^+$GBEC. Magnification = original ×100.

GFP$^+$ Colonies in Recipient SCID Mouse Livers Express the Biliary Epithelial Cell Markers CK19 and Carbonic Anhydrase IV

Normal GBEC express CK19, whereas murine hepatocytes do not. GFP$^+$ colonies with a ductular morphology expressed CK19 to a variable extent (Figure 8). The red stain is specific for CK19, and is found predominantly on the apical surfaces of the epithelial-like cells that are also GFP$^+$. Similar results were seen with the biliary epithelial cell marker carbonic anhydrase IV (data not shown).

GFP$^+$ Colonies in Recipient Mouse Livers Express Hepatocyte Markers

HNF-4α is a transcription factor expressed in the nuclei of hepatocytes (Figure 9A), but not in GBEC nuclei (not shown). Within GFP$^+$ colonies that exhibited mixed histological architecture (as shown in Figures 4 and 5), HNF-4α expression was evident in cells with a hepato-

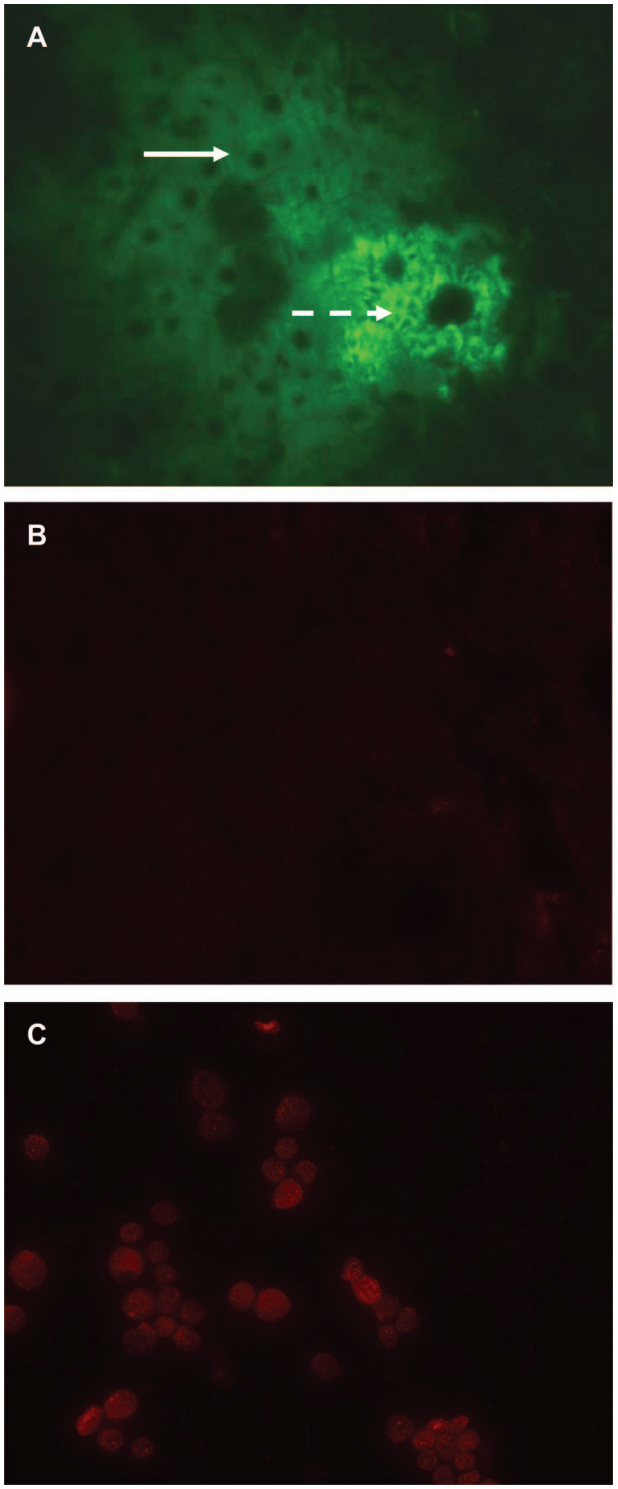

Figure 7. PCNA expression in liver of a SCID mouse, treated as in Figure 2. **A:** A GFP$^+$ colony as seen with FITC filter on fluorescence microscopy. Note the hepatocyte-like morphology of GFP$^+$ cells to the left (**solid arrow**), which contrasts with the epithelial-like GFP$^+$ cells to the right (**dashed arrow**). **B:** Same section as in (**A**) stained with a PCNA antibody. The faint, red fluorescence outside the nuclei is due to autofluorescence. **C:** PCNA immunofluorescence in an actively dividing subconfluent monolayer of wild-type GBEC. Magnification = original ×400.

cyte-like morphology (ie, large round nuclei with broad cytoplasm), but not in cells with an epithelial cell-like morphology (Figure 9, B and C).

Connexin-32 is a plasma membrane protein expressed in hepatocytes but not in GBEC (Figure 10A). Expression in hepatocytes is observed as punctate and linear staining on the cell surface. In recipient mouse liver, a similar pattern of expression was found in GFP$^+$ regions with hepatocyte-like morphology (Figure 10, B and C), but not in GFP$^+$ cells with an epithelial cell-like morphology.

GFP$^+$ cells with large nuclei that were hepatocyte-like in the same vicinity as small GFP$^+$ epithelial cell-like cells that were CK19-positive did not express CK19 (Figure 11). These hepatocyte-like cells expressed HNF-4α and connexin-32 when examined in adjacent GFP$^+$ sections from the same liver. This suggests that hepatocyte-like GFP$^+$ cells were not dead or dying native hepatocytes that might have nonspecifically picked up the GFP stain. This finding also suggests that the hepatocyte-like cells did not possess bipotential characteristics.

Discussion

Our study shows that terminally differentiated GBEC are capable of engrafting and surviving in damaged mouse liver, and that a subpopulation of these engrafted cells develop hepatocyte-like characteristics. Transplanted GBEC, identified by GFP fluorescence, engraft in distinct colonies mostly characterized by vesicles lined with a single layer of small epithelial-like cells that express biliary epithelial cell markers. Some GFP$^+$ colonies contain larger cells that resemble hepatocytes morphologically and express hepatocyte markers. These findings complement our earlier *in vitro* study that had demonstrated the acquisition of phenotypic characteristics of hepatocytes by murine GBEC cultured under specific conditions.[10] Thus, both *in vitro* and *in vivo*, these findings demonstrate that environmental cues are sufficient to reprogram a subpopulation of GBEC into acquiring phenotypic characteristics of hepatocytes. Our results provide a rationale to pursue the possibility of using GBEC as donor cells for liver cell replacement therapy.

The finding of GFP$^+$ cells in recipient livers with morphological and gene expression features of either biliary epithelial cells or of hepatocyte-like cells raises the possibility that the original GBEC population harbored cells with pluripotential stem-cell-like properties that could home to the liver and differentiate into two lineages. Alternatively, the original GBEC donor cell population could harbor two different types of stem cells, with one type destined to differentiate into biliary epithelial cells and the other to differentiate into hepatocyte-like cells. We previously showed that GBEC did not express the hematopoietic and oval cell markers CD34, Sca-1, or α fetoprotein.[10] Furthermore, studies of cell cycle kinetics did not support the presence of a small population of constantly renewing cells.[10] The five key transcription factors that have been shown to induce pluripotential stem cells in mouse and human fibroblasts, Oct3/4, Sox2, c-Myc, Klf4, and Nanog,[20–22] are not expressed in cultured mouse GBEC, as determined by real time PCR (data not shown). If such pluripotential stem cells were to exist at low numbers in isolated GBEC, then isolation, selection, and en-

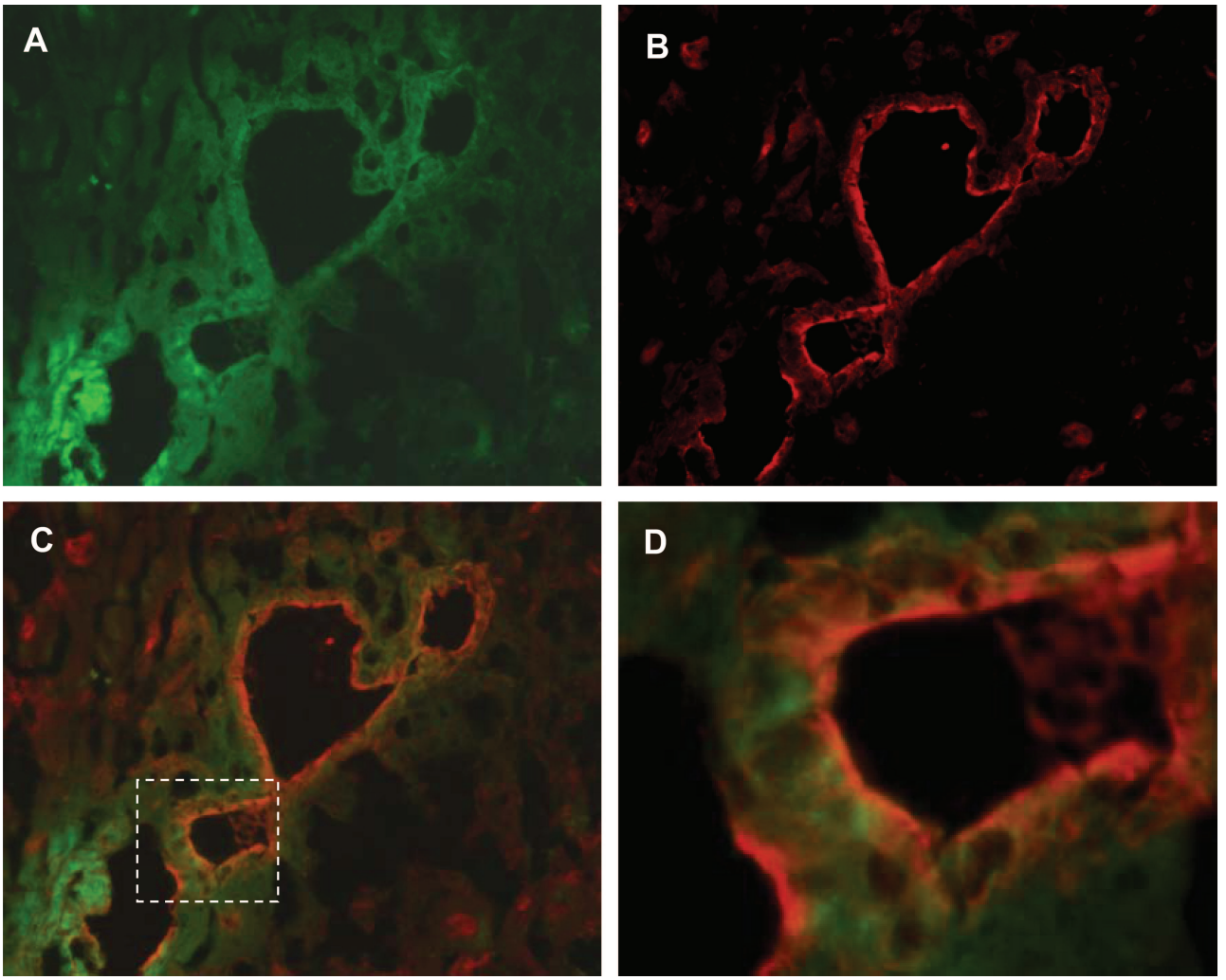

Figure 8. CK19 expression in liver of recipient SCID mouse, treated as in Figure 2. **A:** GFP^+ colony in recipient SCID mouse liver as seen with the FITC filter via fluorescence microscopy. **B:** Same section as in (**A**), stained with an antibody to CK19 and a rhodamine-labeled secondary antibody. **C:** Overlay image showing GFP^+ areas that co-localize with CK19 expressing areas. Magnification = original ×400. **D:** Higher magnification view of the boxed area in (**C**). Similar results were seen in the other treatment groups shown in Table 1, which had engraftment rates ≥50%.

richment of cells destined to differentiate into hepatocyte-like cells before cell transplantation might allow for more efficient engraftment and repopulation of hepatocytes in damaged recipient liver. Neither our *in vitro*[10] or current *in vivo* studies support the presence of cells with stem cell-like properties in the donor GBEC pool.

One mechanism that could explain the *in vivo* findings, but could not have a counterpart in the *in vitro* situation, is that of cell fusion. Previous studies have shown that bone marrow-derived cells that differentiated into various cell types, including hepatocytes, did so via cell fusion.[23–26] If cell fusion were the mechanism for our current *in vivo* findings, then the acquisition of hepatocyte-like characteristics of GBEC in defined culture conditions in our *in vitro* study,[10] in which no recipient hepatocytes were present, must have occurred via a completely different mechanism. In addition, there are no reports in the literature of terminally differentiated extrahepatic biliary epithelial cells, such as GBEC, fusing with native hepatocytes to form hepatocyte-like cells. Nonetheless, we are currently analyzing the possibility that cell fusion occurred *in vivo* by performing transplants of GFP^+GBEC in a sex-mismatched protocol followed by chromosomal analysis.

Transdifferentiation ("reprogramming") of terminally differentiated GBEC into hepatocyte-like cells is a third possible mechanism for our findings. This is the most likely mechanism, since our *in vitro* studies showed the acquisition by GBEC of a spectrum of hepatocyte-like characteristics, and there is no data to support either cell fusion or the presence of pluripotential stem-cell like cells, as noted above. Transdifferentiation of rat hepatocytes into biliary cells occurs after bile duct ligation and toxic biliary injury[4] and *in vitro.*[7] Transdifferentiation of pancreas to liver has also been reported.[8] Thus, the most parsimonious explanation for the finding of hepatocyte-like cells in both our *in vitro*[10] and our *in vivo* studies is that of transdifferentiation. Since GBEC and hepatocytes share a common embryologic origin, we speculate that genetic reprogramming of GBEC into hepatocyte-like cells can occur under suitable environmental conditions. Our data do not prove that donor GBEC that engrafted

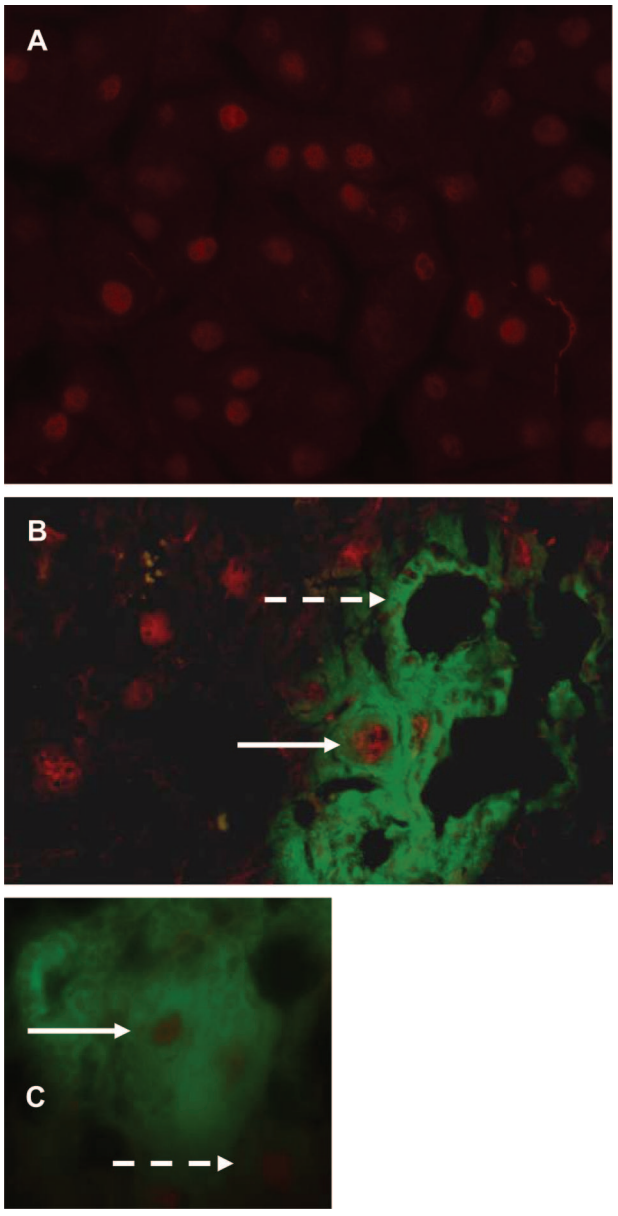

Figure 9. HNF-4α expression in a normal mouse liver and the liver of a recipient SCID mouse, treated as in Figure 2. **A:** HNF-4α expression in normal mouse liver, showing prominent nuclear staining in hepatocytes. **B:** A GFP^+ colony from engrafted mouse, with mixed histological architecture, showing HNF-4α expression in the nucleus of a hepatocyte-like cell (**solid arrow**), but with no HNF-4α expression in cells with an epithelial cell-like morphology (**dashed arrow**). Magnification = original ×400. **C:** GFP^+ colony showing HNF-4α expression in the nucleus of a GFP^+ cell (**solid arrow**). HNF-4α expression is also present in cells that are not GFP^+ (**dashed arrow**), representing native hepatocytes in the recipient liver. Magnification = original ×400. Similar results were seen in the other treatment groups shown in Table 1, which had engraftment rates ≥50%.

into recipient mouse livers *actually* became hepatocytes; rather, our data show that certain engrafted GFP^+ cells acquired certain phenotypic and morphological characteristics that could be described as hepatocyte-like.

Recently, Zhou et al, using adenoviral vector-mediated delivery, showed that the *in vivo* re-expression of three key developmental transcriptional factors was sufficient to reprogram mouse pancreatic exocrine cells into cells

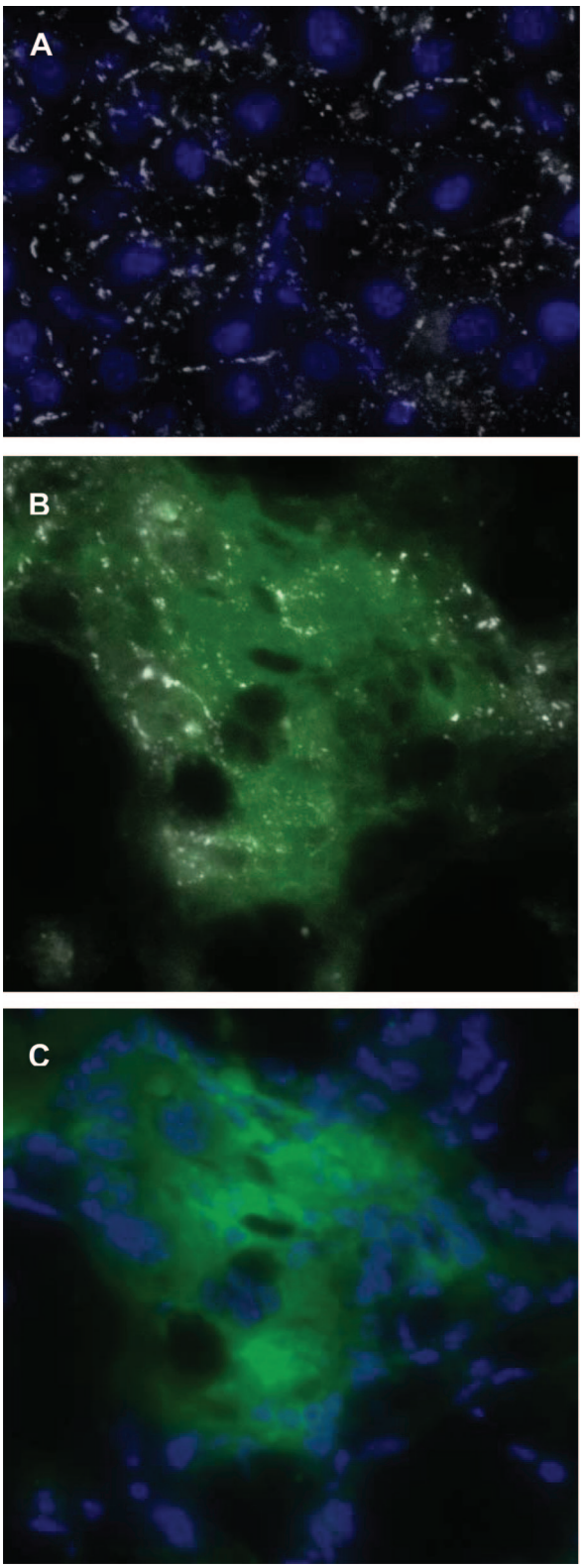

Figure 10. Connexin-32 expression in a normal mouse liver and the liver of a recipient SCID mouse, treated as in Figure 2. **A:** Immunofluorescence image of a section of normal mouse liver stained with an anti-connexin-32 antibody (white) and with a nuclear dye (blue). **B:** A GFP^+ colony in recipient SCID mouse liver (green), overlaid with the same section stained with an anti-connexin-32 antibody (white). **C:** Same section as in (**B**), showing the green fluorescence area with nuclear staining. Magnification = original ×400. Similar results were seen in the other treatment groups shown in Table 1 which had engraftment rates >50%.

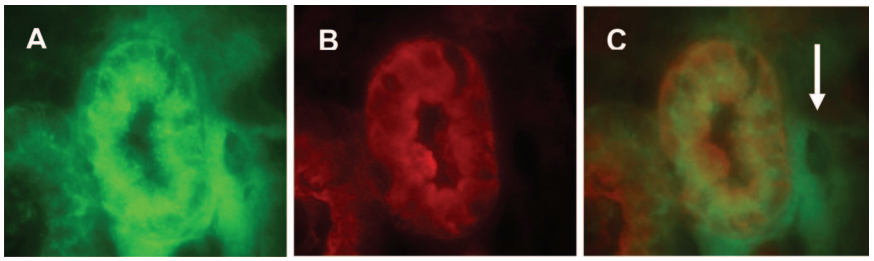

Figure 11. CK19 expression in the liver of a recipient SCID mouse, treated as in Figure 2. **A:** GFP$^+$ colony in recipient SCID mouse liver (green). **B:** Same section as in (**A**) stained with a CK19 antibody. **C:** Overlay image. **Arrow** points to a hepatocyte-like cell that did not express CK19. Magnification = original ×400.

that closely resembled pancreatic β-cells.[27] This principle, that terminally differentiated cells of one type could be made to transdifferentiate to another by direct genetic manipulation, is attracting attention as a means toward one goal of regenerative medicine. Direct genetic manipulation allows for strict control of expression of certain transcriptional factors, but is cumbersome and clinically problematic, given the need to deliver genes using viral vectors. In contrast, our study suggests that direct genetic manipulation might not be necessary; local environmental cues may be sufficient to effect this genetic reprogramming in a subpopulation of donor cells.

Our findings raise a number of questions. First, what is the cellular and molecular basis for the epithelial-like morphology of most of the GFP$^+$ cells and their arrangement in a single layer lining vesicles in recipient mouse livers? The simplest explanation is that the transplanted GBEC are attempting to form gallbladders within the recipient liver. A second, related question pertains to the fluid content of the vesicles, which revealed no proteinaceous material on H&E staining. We speculate that activation of apical plasma membrane transporters and channels in these epithelial cells could mediate secretion of fluid and electrolytes into the vesicles, mimicking the apical plasma membrane functions found in GBEC.

Another set of questions relates to the identity of the GFP$^+$ cells within the engrafted colonies. Are there a spectrum of cells with varying degrees of differentiation ranging from GBEC to hepatocyte-like cells, or are there two or more distinct cell populations? There appears to be at least two distinct cell populations: Small, columnar epithelial cells that line the vesicles and express only biliary epithelial cell markers, such as CK19; and larger, hepatocyte-like cells that express only hepatocyte markers, such as HNF-4α. Since only four areas were examined on each of four sections from each liver, we cannot exclude that some engrafted cells express both biliary and hepatocyte markers. More detailed characterization of the engrafted cells will need to be performed to address this issue. What are the gene expression profiles of these cells, and what are their relative contributions to survival and propagation within the engrafted colonies? Our *in vitro* work suggests that murine GBEC are capable of differentiating into hepatocyte-like cells through a spectrum of changes in gene expression, with certain hepatocyte genes being expressed.[10] Further work needs to be done to better characterize the cells in the GFP$^+$ colonies to determine to what extent the *in vitro* findings can be translated to the *in vivo* situation. Are these engrafted cells potentially neoplastic, or could the predominant vesicular structures accumulate fluid and expand within the liver (resembling Caroli's disease)? This is unlikely, since PCNA staining indicated that they do not actively proliferate, and the GFP$^+$ colonies remained stable in size and appearance over the 4-month time frame of our studies. Analysis at longer time points would be necessary to determine the long-term fate of the engrafted cells.

Another important question is whether the transplanted cells are capable of functionally replacing hepatocytes in a clinically relevant manner. The percentage of engrafted cells was low (especially as compared with data derived from the extensive work done with hepatocyte transplantation in various animal models[11,13–17]). In addition, hepatocyte-like cells were in the minority in the colonies, and there was no evidence that they were proliferating. Our study represents a proof-of-concept, and the preceding limitations might be improved with refinements in the protocol. This technique of engraftment might not be sufficiently robust for patients with end stage liver disease, in whom a myriad of hepatocyte functions must be replaced. However, for replacement of specific deficiencies in hepatic enzyme or protein synthesis (eg, factor IX in patients with hemophilia), relatively small numbers of engrafted cells that acquired this capability could provide therapeutic benefit. These questions can be addressed by future studies of transplantation into mouse livers of GBEC that have been transduced with viral vectors carrying appropriate therapeutic target genes.

In summary, we have demonstrated for the first time that well-differentiated epithelial cells derived from the extra-hepatic biliary system are capable of engrafting and surviving in damaged mouse liver. Our discovery that subpopulations of donor cells acquire phenotypic characteristics that can be described as hepatocyte-like suggests that terminally differentiated cells of the extra-hepatic biliary system have the capability to transdifferentiate into a hepatocyte-like cell in the appropriate environment. These findings raise the possibility of a future clinical use for GBEC as donor cells in a cell transplantation protocol for the treatment of liver diseases.

Acknowledgments

We thank Drs. J. Donald Ostrow and Jeffrey Virgin for critical review of the manuscript.

References

1. Fausto N: Liver regeneration. J Hepatol 2000, 32:19–31
2. Alison MR, Vig P, Russo F, Bigger BW, Amofah E, Themis M, Forbes S: Hepatic stem cells: from inside and outside the liver? Cell Prolif 2004, 37:1–21
3. Fausto N: Liver regeneration and repair: hepatocytes, progenitor cells, and stem cells. Hepatology 2004, 39:1477–1487
4. Michalopoulos GK, Barua L, Bowen WC: Transdifferentiation of rat hepatocytes into biliary cells after bile duct ligation and toxic biliary injury. Hepatology 2005, 41:535–544
5. Sell S: Heterogeneity and plasticity of hepatocyte lineage cells. Hepatology 2001, 33:738–750
6. Sirica AE, Williams TW: Appearance of ductular hepatocytes in rat liver after bile duct ligation and subsequent zone 3 necrosis by carbon tetrachloride. Am J Pathol 1992, 140:129–136
7. Nishikawa Y, Doi Y, Watanabe H, Tokairin T, Omori Y, Su M, Yoshioka T, Enomoto K: Transdifferentiation of mature rat hepatocytes into bile duct-like cells in vitro. Am J Pathol 2005, 166:1077–1088
8. Shen CN, Slack JM, Tosh D: Molecular basis of transdifferentiation of pancreas to liver. Nature Cell Biol 2000, 2:879–887
9. Beresford WA: Direct transdifferentiation: can cells change their phenotype without dividing? Cell Differ Dev 1990, 29:81–93
10. Kuver R, Savard CE, Lee SK, Haigh WG, Lee SP: Murine gallbladder epithelial cells can differentiate into hepatocyte-like cells in vitro. Am J Physiol Gastrointest Liver Physiol 2007, 293:G944–G955
11. Rhim JA, Sandgren EP, Degen JL, Palmiter RD, Brinster RL: Replacement of diseased mouse liver by hepatic cell transplantation. Science 1994, 263:1149–1152
12. Chamberlain J, Yamagami T, Colletti E, Theise ND, Desai J, Frias A, Pixley J, Zanjani ED, Porada CD, Almeida-Porada G: Efficient generation of human hepatocytes by the intrahepatic delivery of clonal human mesenchymal stem cells in fetal sheep. Hepatology 2007, 46:1935–1945
13. Stephenne X, Najimi M, Sibille C, Nassogne MC, Smets F, Sokal EM: Sustained engraftment and tissue enzyme activity after liver cell transplantation for argininosuccinate lyase deficiency. Gastroenterology 2006, 130:1317–1323
14. Lee KW, Lee JH, Shin SW, Kim SJ, Joh JW, Lee DH, Kim JW, Park HY, Lee SY, Lee HH, Park JW, Kim SY, Yoon HH, Jung DH, Choe YH, Lee SK: Hepatocyte transplantation for glycogen storage disease type Ib. Cell Transplant 2007, 16:629–637
15. Strom SC, Bruzzone P, Cai H, Ellis E, Lehmann T, Mitamura K, Miki T: Hepatocyte transplantation: clinical experience and potential for future use. Cell Transplant 2006, 15:S105–S110
16. Grompe M: Principles of therapeutic liver repopulation. J Inherit Metab Dis 2006, 29:421–425
17. Nagata H, Nishitai R, Shirota C, Zhang JL, Coch CA, Cai J, Awwad M, Schuurman HJ, Christians U, Abe M, Baranowska-Kortylewidz J, Platt JL, Fox IJ: Prolonged survival of porcine hepatocytes in cynomolgus monkeys. Gastroenterology 2007, 132:321–329
18. Kuver R, Savard C, Nguyen TD, Osborne WR, Lee SP: Isolation and long-term culture of gallbladder epithelial cells from wild-type and CF mice. In Vitro Cell Dev Biol Animal 1997, 33:104–109
19. Laconi E, Oren R, Mukhopadhyay DK, Hurston E, Laconi S, Pani P, Dabeva MD, Shafritz DA: Long-term, near-total liver replacement by transplantation of isolated hepatocytes in rats treated with retrorsine. Am J Pathol 1998, 153:319–329
20. Okita K, Ichisaka T, Yamanaka S: Generation of germline-competent induced pluripotent stem cells. Nature 2007, 448:313–317
21. Wernig M, Meissner A, Foreman R, Brambrink T, Ku M, Hochedlinger K, Bernstein BE, Jaenisch R: In vitro reprogramming of fibroblasts into a pluripotent ES-cell-like state. Nature 2007, 448:318–324
22. Takahashi K, Tanabe K, Ohnuki M, Narita M, Ichiska T, Tomoda K, Yamanaka S: Induction of pluripotent stem cells from adult human fibroblasts by defined factors. Cell 2007, 131:861–872
23. Alvarez-Dolado M Pardal R, Garcia-Verdugo JM, Fike JR, Lee HO, Pfeffer K, Lois C, Morrison SJ, Alvarez-Buylla A: Fusion of bone-marrow-derived cells with Purkinje neurons, cardiomyocytes and hepatocytes. Nature 2003, 425:968–973
24. Terada N, Hamazaki T, Oka M, Hoki M, Mastaleerz DM, Nakano Y, Meyer EM, Morel L, Petersen BE, Scott EW: Bone marrow cells adopt the phenotype of other cells by spontaneous cell fusion. Nature 2002, 416:542–545
25. Vassilopoulos G, Wang PR, Russell DW: Transplanted bone marrow regenerates liver by cell fusion. Nature 2003, 422:901–904
26. Wang X, Willenbring H, Akkari Y, Torimaru Y, Foster M, Al-Dhalimy M, Lagasse E, Finegold M, Olson S, Grompe M: Cell fusion is the principal source of bone-marrow-derived hepatocytes. Nature 2003, 422:897–901
27. Zhou Q, Brown J, Kanarek A, Rajagopal J, Melton DA: In vivo reprogramming of adult pancreatic exocrine cells to b-cells. Nature 2008, 455:627–632